Pilot Study

Predictive Clinical Decision Support System Using Machine Learning and Imaging Biomarkers in Patients With Neurostimulation Therapy: A Pilot Study

Jose De Andres, MD, PhD[1,2], Amadeo Ten-Esteve, Ing[3], Anushik Harutyunyan, PsychD[2], Carolina S. Romero-Garcia, MD, PhD[2,4], Gustavo Fabregat-Cid, MD, PhD[2], Juan Marcos Asensio-Samper, MD[2], Angel Alberich-Bayarri, Ing[3,5], and Luis Marti-Bonmati, MD, PhD[3,6]

From: [1]Anesthesia Unit-Surgical specialties Department, Valencia University Medical School, Valencia, Spain; [2]Multidisciplinary Pain Management Department, Department of Anesthesiology, Critical Care and Pain Management, General University Hospital, Valencia, Spain; [3]Biomedical Imaging Research Group (GIBI230-PREBI) at La Fe Health Research Institute, and Imaging La Fe node at Distributed Network for Biomedical Imaging (ReDIB) Unique Scientific and Technical Infrastructures (ICTS), Valencia, Spain; [4]Universidad Europea Valencia, Spain; [5]Quantitative Imaging Biomarkers in Medicine, QUIBIM SL, Valencia, Spain; [6]La Fe University and Polytechnic Hospital, Valencia, Spain

Address Correspondence:
Jose De Andres, MD, PhD
Department of Anesthesia, General University Hospital Consortium of Valencia: Avda. Tres Cruces s/n
Valencia, Spain 46014
E-mail: deandres_jos@gva.es

Disclaimer: There was no external funding in the preparation of this manuscript.

Conflict of interest: Each author certifies that he or she, or a member of his or her immediate family, has no commercial association (i.e., consultancies, stock ownership, equity interest, patent/licensing arrangements, etc.) that might pose a conflict of interest in connection with the submitted manuscript.

Manuscript received: 06-29-2021
Revised manuscript received: 08-22-2021
Accepted for publication: 08-31-2021

Free full manuscript: www.painphysicianjournal.com

Background: Chronic pain is correlated with alterations in brain structure and function. The selection process for the ideal candidate for spinal cord stimulation (SCS) therapy is based on functional variables analysis and pain evaluation scores. In addition to the difficulties involved in the initial selection of patients and the predictive analysis of the trial phase, the large rate of explants is one of the most important concerns in the analysis of the suitability of implanted candidates.

Objective: To investigate the usefulness of imaging biomarkers, functional connectivity (FC) and volumetry of the whole brain in patients with Failed back surgery syndrome (FBSS) and to create a clinical patient-based decision support system (CDSS) combining neuroimaging and clinical data for predicting the effectiveness of neurostimulation therapy after a trial phase.

Study Design: A prospective, consecutive, observational, single center study.

Setting: The Multidisciplinary Pain Management Department of the General University Hospital in Valencia, Spain.

Methods: A prospective, consecutive, and observational single-center study. Using Resting-state functional magnetic resonance imaging (rs-fMRI) and Region of interest (ROI) to ROI analysis, we compared the functional connectivity between regions to detect differences in FC and volume changes. Basal magnetic resonance images were obtained in a 1.5T system and clinical variables were collected twice, at the basal condition and at 6-months post-SCS implant. We also conducted a seed-to-voxel analysis with 9 items as seed-areas characterizing the functional connectivity networks. A decreased in 10 units in the Pain Detect Questionnaire (PD-Q) score was established to define the subgroup of Responders Group (R-G) to neurostimulation therapy. The clinical variables collected and the imaging biomarkers obtained (FC and volumes) were tested on a set of 6 machine learning approaches in an effort to find the best classifier system for predicting the effectiveness of the neurostimulator.

Results: Twenty-four patients were analyzed and only seven were classified in the R-G. Volumetric differences were found in the left putamen, $F = 34.06$, $P = 0.02$. Four pairwise brain areas showed statistical differences in the rs-fMRI including the right insular cortex. Linear Discriminant Analysis showed the best performance for building the CDSS combining clinical variables and significant imaging biomarkers, the prediction increased diagnostic accuracy in the R-G patients from 29% in current practice to 96% of long-term success.

Conclusion: These findings confirm a major role of the left putamen and the four pairs of brain regions in FBBS patients and suggest that a CDSS would be able to select patients susceptible to benefitting from SCS therapy adding imaging biomarkers

Key words: Chronic pain, failed back surgery syndrome, neuroimaging, imaging biomarker, machine learning, rs-fMRI, spinal cord stimulation, structural imaging, supraspinal mechanisms

Pain Physician 2021: 24:E1279-E1290

Chronic pain management is a great challenge for physicians worldwide. Spinal cord stimulation (SCS) therapy is indicated in multidisciplinary pain departments when other therapies have failed (1-7). The selection criteria for SCS eligibility are based on an interaction of clinical and psychosocial factors (4), and on the costs and benefits of the implanted system (8). Guidelines are not explicit enough and subjectivity plays an important role in addressing the increasing heterogeneity of patients who might be candidates for SCS.

Traditionally, the trial phase of an SCS therapy (9,10) is carried out to identify patients who would benefit from the definitive implant by evaluating the level of global improvement obtained (11). When the pain intensity decreases by more than 50% as measured using the numeric rating scale (NRS), a definitive SCS implant will be proposed (9). Also, one in 2 patients will have long-term failure depending on the rate of false positives and false negatives in the subjective trial phase and even in a single-stage (9,10) implantation plan. In addition, the efficacy of SCS implants after a successful trial phase decreases significantly in the following 4 years (12), which complicates the selection of the right patient for the SCS system (10,11,13,14). Patel et al (15) described a failure of the system that led to device removal in 81% of patients due to lack of effectiveness. The patient´s personal goals and the global level of satisfaction experienced were other factors determining SCS therapy outcomes (16). Thus, clinical practice reinforces the need to further investigate the patient´s phenotypes to predict SCS adequate response (17). Functional magnetic resonance (fMR) studies have described a positive association between pain duration and connective brain alterations (18-20). Particularly, patients with chronic pain showed functional and structural brain alterations in resting-state functional magnetic resonance imaging (rs-fMRI) (18,19,21) on failed back surgery syndrome (FBSS). Recent studies highlight the usefulness of combining imaging biomarkers and machine learning techniques for the discrimination of patients with chronic low back pain (22). Nevertheless, the applicability of such models in the appropriate selection of the patients that will benefit from SCS therapy remains unexplored. The hypothesis of this study is that the inclusion of structural and quantitative information from rs-fMRI might help with the selection of patients who would benefit from SCS therapy. Our aim was to analyze the neuronal networks involved in FBSS and create a clinical decision support system (CDSS) to predict SCS response before implantation. Different classifier approaches have been employed in this study on the most relevant image biomarkers and clinical variables. These classifiers, within artificial intelligence, belong to the subclass of supervised machine learning. The objective is to have a system capable of learning and discriminating between patient populations for which the experience and judgment of clinicians currently encounter great difficulties.

Methods

Study Design

We performed a pilot observational and single-center study in the Multidisciplinary Pain Management Department of the General University Hospital in Valencia from November 31, 2016, to June 12, 2019. The workflow proposed is represented schematically in Fig. 1. The Institutional Review Board approved the study on July 14th, 2016, and written informed consent was obtained from all patients. A CDSS system was created and we adhered to the standards for reporting diagnostic accuracy studies (STARD) (23). Also registered in ClinicalTrials.gov with Identifier: NCT04735159.

Patients

A total of 32 patients who had an FBSS diagnosis (3) and treated with SCS implants were consecutively enrolled for the study. The inclusion criteria were pain lasting longer than 6 months, basal NRS $\geq$ 5. The exclusion criteria were psychiatric diseases or significant cognitive or psychological deficits diagnosed using the DSM-IV (24) and the American Society Anesthesiologists physical status classification ASA $\geq$ III, the lack of improvement during the trial phase (3 patients) and the presence of artifacts in the rs-fMRI (5 patients). Thus, the final sample size was 24 patients. All patients have tonic stimulation and were implanted with 2 AvistaTM 8-pole electrodes, and Generator MontageTM.(Boston Scientific Corporation. Valencia, CA, USA). Strict protocolization of the programming of all the patients included in the study, was applied, using Illumina 3D algorithm™, to eliminate the individual variation and related influence in the results (Appendix 1).

Self-Reported Measures

Clinical variables were obtained at the baseline and 6 months after SCS implantation (Table 1), while rs-fMRI images were obtained only at baseline. Included sociodemographic data is shown in Table 2.

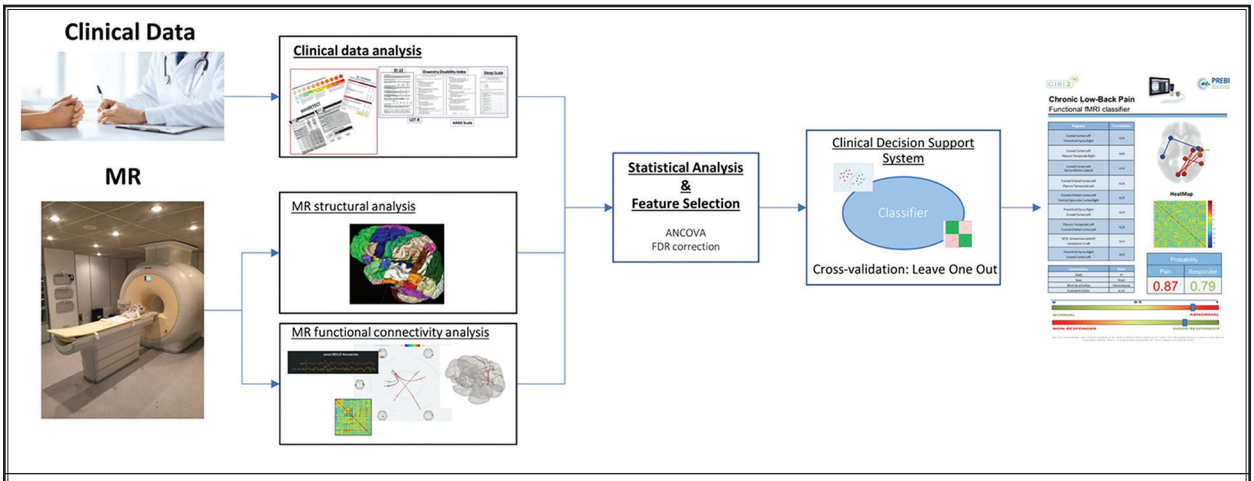

Fig. 1. *Methodology used for the creation of the clinical decision support system based on clinical variables together with morphological and functional brain imaging biomarkers to maximize the success of the SCS implantation.*

Self-reported measures such as anxiety and depression were assessed with the Hospital Anxiety and Depression Score (HADS). Resilience was measured with the 10-item Connor-Davidson Resilience Scale (CD-RISC10) questionnaire. Also, we collected the 12-item Medical Outcomes Study Social Support Survey (MOS-SS) questionnaire to obtain the mean number hours of sleep per day. To measure pain, the NRS of pain and the Pain Detect Questionnaire (PD-Q) were recorded. Other variables included in clinical practices were the percentage of body area covered by the neurostimulator, and the level of satisfaction with the treatment. If the patient reported any side effects, these were registered in the electronic medical record.

Table 1. *Evolution of clinical variables before and after neurostimulation therapy.*

Variables	Basal	6-months post implant	*P* value
NRS	7.5 (2.3)	5.6 (2.6)	< 0.05
PD-Q	20.2 (6.2)	13.6 (8.1)	< 0.05
MOS-SS (hours of sleep)	6.4 (1.9)	6.5 (1.3)	0.87
HADS - Anxiety	10.7 (3.8)	6.8 (4.7)	0.11
HADS- Depression	7.9 (3.8)	6.8 (6.1)	0.23
Resilience	28.1 (7.7)	27.7 (10.3)	0.74

Variables are expressed as means and standard deviation (SD). NRS, Numeric rating scale; PD-Q, Pain detect questionnaire; MOS-SS, Medical outcomes study social support survey; HADS, Hospital anxiety and depression score.

MRI Data Acquisition

Magnetic resonance (MR) images were obtained using the 1.5T MR system (Ingenia, Philips, Best, The Netherlands) with 8-channel head coil according to the approved settings/recommendations for SCS devices (Appendix 2).

Transverse brain images were acquired parallel to the anterior commissure and posterior commissure plane with the following sequences:

T1 weighted high-resolution gradient echo (HR-GRE) sequence (3D-T1w-HR-GRE): TE/TR = 4.6/9.5 ms, voxel size = 0.48 x 0.48 x 1.00 mm, acquisition matrix = 512 x 512 x 170, flip angle = 16°. These images were used to parcellate brain regions and for the voxel-base morphometry (VBM) analysis.

rs-fMRI was obtained by blood oxygenation level–dependent (BOLD) sequence imaging with a T2* weighted Echo Planar Imaging (EPI) sequence with continuous acquisition: TE/TR = 50 / 2750 ms, voxel dimensions = 3.59x3.59 x 4 mm, acquisition matrix = 64 x 64 x 30, dynamic blocks = 135, total acquisition time was 6-minutes. The patients were instructed to keep their eyes close during all the sequence acquisition.

Quantitative Image Analysis

Both T1 weighted gradient echo (T1w-GRE) and rs-fMRI sequences were initially processed using the CONN toolbox (www.nitrc.org/projects/conn, RRID:SCR_009550) and SPM8 (Wellcome Trust Center for Neuroimaging, University College London, London, UK) software tools.

The rs-fMRI connectivity analysis pipeline consisted of an initial pre-processing including realignment, un-

Table 2. *Basal characteristics of the responders group (R-G) and the non-responder group (NR-G) based on a decreased of more than 10 units in the Pain-Detect Questionnaire (PD-Q).*

Clinical Variables	**R-Group 7 patients**	**NR-Group 17 patients**	***P* value**
Age	49 (1)	49 (6)	n.s
Gender	57% F	49% F	n.s
Civil Status Married Divorce Single	 71% (14) 14% (1) 14% (1)	 82% (5) 9% (1) 9% (1)	n.s
Scholarship Intermediate Elementary Superior University	 41 % (12) 24 % (2) 24 % (2) 11 % (1)	 14% (1) 43% (3) 29% (2) 14% (1)	n.s
NRS	7.2 (2.3)	7.5 (2.5)	n.s
HADS - Anxiety	12.9 (4.5)	6.8 (4.7)	n.s
HADS- Depression	7.6 (4.0)	6.8 (6.1)	n.s
MOS-SS (hours of sleep per day)	5.6 (1.3)	6.6 (1.2)	n.s
Resilience	30.1 (4.8)	27.7 (10.3)	n.s
PD-Q	24.3 (2.8)	18.2 (6.3)	0.03
Imaging biomarkers variables	**R-G 7 patients**	**NR-G 17 patients**	***P* value**
I. FC between right anterior division of the inferior temporal gyrus and right frontal operculum cortex	0.16 (0.17)	-0.01 (0.13)	0.04
II. FC between left planum temporale and right insular cortex	0.18 (0.16)	0.34 (0.22)	0.03
III. FC between precentral gyrus and left temporooccipital part of the inferior temporal gyrus	0.17 (0.20)	0.01 (0.19)	0.02
IV. FC left anterior division of the supramarginal gyrus and left precentral gyrus	0.11 (0.07)	0.02 (0.19)	0.04
Volume of left putamen	0.20 (0.01)	0.22 (0.02)	0.02

Variables are expressed as means and standard deviation (SD). NRS, numeric rating scale; PD-Q, pain detect questionnaire; MOS-SS, medical outcomes study social support survey (hours of sleep per day); HADS, hospital anxiety and depression score; CD-RISC10, Connor-Davidson Resilience Scale (Resilience); FC, functional connectivity; n.s: not significant.

wrapping, movement estimation, and outlier exclusion. Functional images were registered to the structural ones for each subject using rigid deformation (21,22,25,26). Finally, they were normalized to the Montreal Neurological Institute (MNI) geometrical space, to overlay the Harvard-Oxford probabilistic brain atlas and determine the regions of interest (ROI). The pre-defined ROI were used to identify the main cortical (91 regions) and subcortical (15 regions) brain areas. Seed-areas (9 items) characterizing the known functional connectivity networks (Default Mode Network, Dorsal Attention Network, Salience Network, Sensory Motor Network, Visual Network, Dorsal Attention Network, Fronto-Parietal Network, Language Network, and Cerebellar Network) were also considered.

For every pairwise region identified with the Harvard-Oxford probabilistic atlas, the correlation coefficients were calculated after removal of the non-neural blood oxygenation level-dependent (BOLD) fluctuations. To calculate the ROI-to-ROI correlations, we used automatic low-frequency fluctuation methods, which yielded correlation matrices to show the correlation values (CONN v.17, Functional Connectivity SPM toolbox; McGovern Institute of Brain Research, Massachusetts Institute of Technology) to detect differences between patient groups.

Clinical Decision Support System (CDSS)

To assess the success or failure of the SCS, we predefined a cut-off point of at least an improvement of 10 units (≥ 30% of the total score) in the PD-Q at 6 months compared to the basal level based on the sub-

jective clinical experience of the physicians working in the multidisciplinary pain unit. A subset of the sample has allocated patients as follows. If SCS therapy was not successful, patients were placed in the nonresponders group (NR-G), while if the SCS device improved neuropathic pain as defined above, patients were placed in the responders group (R-G). CDSS aims to predict a successful outcome in SCS implantation. A pool of 6 classification algorithms based on machine learning were evaluated with Scikit-learn machine learning library in 3 scenarios (27). The difference between scenarios is given by the variables used to train the classifiers: Scenario 1) clinical variables alone; Scenario 2) imaging biomarkers alone; and Scenario 3) combination of clinical variables and imaging biomarkers. The machine learning algorithms evaluated were LR: Logistic Regression; DT: Decision Trees; LDA: Linear Discriminant Analysis; GNB: Gaussian Naive Bayes; KNN: K-neighbors and SVM: Support Vector Machine. Imaging biomarkers were selected from volumetric measures and functional connectivity patterns with statistically significant differences. A cross validation technique without back propagation was employed, due to the limited number of available patients; the leave-one-out method was chosen to maximize the robustness of the classifier evaluation (22,28-31). Because the size of the 2 populations is shown to be unbalanced, the accuracy alone could be overestimating the classifier's ability, so for the classifier with higher accuracy, the confusion matrix was plotted and in order to obtain the precision-recall and sensitivity-specificity metrics to fully characterize the classifier's performance (32,33).

Statistical Analysis

Under the premise that there could be volumetric and functional changes between patients who improved after SCS implant and those who did not, it was necessary to perform a statistical analysis to determine whether these changes exist, removing the influence of other factors such as age, gender, marital status, schooling, anxiety, depression, sleep hours, resilience, NRS, and the PD-Q basal. A one-way analysis of covariance (ANCOVA) control analysis was performed. To adjust for multiple testing, the false discovery rate (FDR) method was applied to adjust the *P* values in order to keep the original significance level of the single test. The p-FDR obtained is the new *P* value after correction by multiple tests (p-FDR < 0.05) (34). The statistical package used was (CONN v.17, Functional Connectivity SPM toolbox; McGovern Institute of Brain Research, Massachusetts Institute of Technology) for second-level analysis ROI-to-ROI FC measures (21) and Pingouin with Scikit-learn: Machine Learning in Python (27,35) for volumetric statistical analysis and classifier evaluation using leave-one-out cross validation technique.

Results

Among the 24 patients, only 7 patients (29%) had an improvement of more than 10 units in the NP-Q. The mean age was 48 (8) years old, and 12 patients (52%) were female. The number of years of pain experienced after surgery was 8 (6). The data of the programming were in average and range (lower and upper): Amplitude (mAmp): 5.92 (1.6-12.5); Pulse Width (μsg): 489.19 (120-850); Rate: (Hz) 48.11 (40-100). Table 2 shows the basal characteristics of the sample and the clinical evolution measured at 6 months post-SCS implant.

The level of satisfaction was good or excellent in 15 patients (61%) at 6 months post-implant and the correspondence with the percentage of neurostimulation coverage of the target area of pain was 75% (25) of the body surface. Finally, the side effects reported were present in 4 patients (16%) at 6 months and were related to battery malfunction, wire displacement, and infection. In the 6-month follow-up visit, 17 patients (72%) answered that they would still choose to reimplant the system to control their symptoms.

According to the preestablished value of a decrease of at least 10 units in the PD-Q score, only 7 patients (29%) were classified in the R-G in current clinical practice and had a mean value of 24.3 (2.8), while the NR-G had a mean value of 18.2 (6.2). The long-term success with clinical variable scores allocated 17 patients (54%) to the NR-G. Furthermore, 7 patients (100%) of the R-G had a PD-Q basal score of more than 18, while in the NR-G, 8 patients (47%) had a result of 18 or less. When pain was assessed with the NRS scale, only 1 patient (18%) in the R-G had a basal pain of 3 out of 10 (and a DP-Q level of 24); the 6 remaining patients reported having more than a 5/10 level of pain. In contrast, the NR-G had a more dispersed distribution of NRS basal pain level, with 3 patients (18%) reporting NRS levels of 5/10 (and a DP-Q level of 6, 12, and 20). Table 2 shows the comparisons of clinical and radiological variables between the 2 groups and the variables used to design the CDSS. Figure 2 shows the connectome ring obtained for the 4 pairs of regions in the ROI-to-ROI analysis and the volumetric differences obtained for each region.

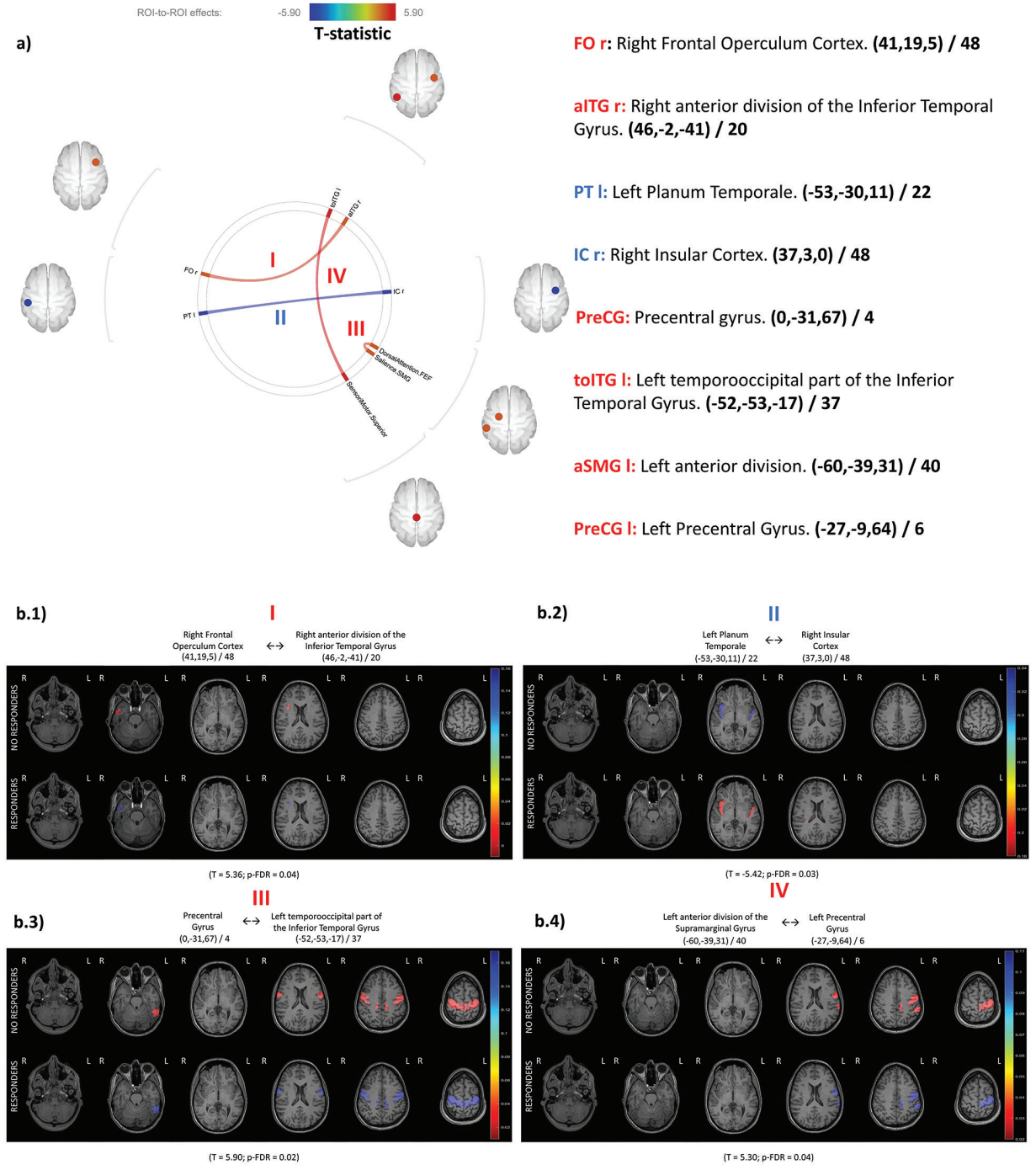

Fig. 2. *Region of interest (ROI)- to-ROI analysis of the 4 pair wise regions with differences in the responder group (R-G) and in the non-responder group (NR-R). Fig 2.a) Conectome ring. Fig 2.b.1), Fig 2.b.2), Fig 2.b.3), and Fig 2.b.4) show the four pair wise regions in the Magnetic resonance (MR) comparing the R-G and the NR-G patients.*

Imaging Biomarkers With rs-fMRI

Brain areas were compared in the respondent group (R-G) and the non-respondent group (NR-G) after the trial phase. Table 3 describes the brain areas that showed statistically significant differences in the functional connectivity analysis:

I (Fig. 2a) The right anterior division of the inferior temporal gyrus (Brodmann´s area 20) showed an inverse correlation (P = 0.04), with the right cortex frontal operculum (Brodmann´s area 48) in patients who did not show improvement of at least 10 units on the PD-Q, while in patients with improvement in the PD-Q of at least 10 units, a positive correlation was shown.

II (Fig. 2b) The left planum temporale (Brodmann´s area 22) with the right insular cortex (Brodmann´s area 48) showed a positive correlation (P = 0.03). The correlation was higher in patients who did not show improvement of at least 10 units on the PD-Q.

III (Fig. 2c) The precentral gyrus (superior sensorimotor network, Brodmann´s area 4) showed a positive correlation with the left temporooccipital part of the inferior temporal gyrus (Brodmann´s area 37) (P = 0.02).

IV (Fig. 2d) The left anterior division of the supramarginal gyrus (salience network, Brodmann´s area 40) with the left precentral gyrus (Brodmann´s area 6) belongs to the dorsal attention network (P = 0.04). In both cases, the correlation was higher in patients who improved at least 10 units.

In the volumetric image analysis, only the left putamen was statistically different with a F = 34.06, P = 0.02 and it showed a volume of 0.20% of the total brain volume in the R-G and a volume of 0.22% in the NR-G.

Clinical Decision Support Systems

The 18 classifiers based on 6 machine learning algorithms in the 3 scenarios: 1) clinical variables alone, 2) imaging biomarkers alone, and 3) combination of clinical variables and imaging biomarkers were built as described in section 2.6. The clinical variables (age, gender, civil status, scholarship, NRS, PD-Q, HADS-anxiety, HADS-depression, and hours of sleep) and imaging biomarkers used for each of the 3 scenarios are those summarized in Table 2 and 3, respectively. The accuracy of each classifier as shown in Table 4. Of 24 patients chosen with the current decision flow as candidates to benefit from SCS treatment, only 7 (29.1%) have responded satisfactorily to SCS, while the best CDSS using clinical variables was 71% and it increased up to 75% when only the imaging biomarkers were applied. Using the combination of clinical and imaging biomarkers, a 95.83% of accuracy was obtained (Fig. 3).

For the best CDSS, LDA using clinical variables and imaging biomarkers, the positive predictive value obtained was 100% and the negative predictive value was 94%. The overall performance of the model had a precision of 92% and the diagnostic accuracy was 96%. Figure 4 summarize the fully characterized performance of the best CDSS obtained.

Table 3. *Functional connectivity differences in the nonresponders group (NR) vs in the responders (R) group . Results from the ROI-to-ROI (region of interest) analysis. ROI 1 and ROI 2 form the pair of regions among which a statistically significant connectivity has been found. Columns 2 and 4 indicate the Montreal Neurological Institute (MNI) coordinates that allow spatial location of the regions and the associated Broadman Area to which they belong. Average correlation value between the pair of regions for patients R-G and the NR-G expressed as means and the T statistics showing the normalized distance between groups. Brodmann´s areas were extracted from the Brodmann´s Interactive Atlas. P values are expressed after the multiple test correction method (P-FDR, False discovery rate method).*

ROI 1	MNI / Brodmann Area	ROI 2	MNI / Brodmann Area	Mean R-Group	Mean NR-Group	T	*P*
Precentral gyrus belongs to the superior sensorimotor network	(0, -31, 67) / 4	Left temporooccipital part of the inferior temporal gyrus	(-52,- 53, -17) / 37	0,17	0,01	5.90	0.02
Left planum temporale	(-53, -30, 11) / 22	Right insular cortex	(37, 3, 0) / 48	0,18	0,34	-5.42	0.03
Right anterior division of the inferior temporal gyrus	(46, -2, -41) / 20	Right frontal operculum cortex	(41, 19, 5) / 48	0,16	-0,01	5.36	0.04
Left anterior division of the supramarginal gyrus belongs to the salience network	(-60, -39, 31) / 40	Left precentral gyrus belongs to the dorsal attention network	(-27, -9, 64) / 6	0,11	0,02	5.30	0.04

Discussion

In this study, we have developed a CDSS to improve patient selection for neurostimulation therapy, based on the results obtained in 24 patients with FBSS, and combined clinical variables and imaging biomarkers. The results obtained are the result of a pilot study with a limited population of patients. Still, the importance of the methodology employed lies in the fact that it offers a promising alternative for mass screening of patients by MRI before implantation of neurostimulators that will improve the estimation of implant success, making it possible to anticipate possible implant failure, and to seek alternatives that will enhance patient management.

Table 4. *Accuracy obtained for pool classifiers test for each CDSS approach.*

Machine Learning Algorithm	Clinical Variables (Accuracy %)	Imaging Biomarkers (Accuracy %)	Clinical Variables & Imaging Biomarkers (Accuracy %)
LR	70.83	70.83	66.66
LDA	54.16	70.83	95.83*
KNN	66.66	62.5	66.66
DT	58.33	66.66	66.66
GNB	66.66	75*	75
SVM	71.00*	66.66	70.83

LR, Logistic Regression; DT, Decision Trees; LDA, Linear Discriminant Analysis; GNB, Gaussian Naive Bayes; KNN, K-neighbors; SVM, Support Vector Machine; *the best approach for each scenario.

In adequate candidates, the SCS implant provides relief in patients with long-lasting neuropathic pain (36). Among different systematic reviews evaluating the response to SCS in FBSS patients, Frey et al (37) concluded that the level of evidence was II 1 or II 2 for long-term use. In addition, Amirdelfan et al (38) reported an evidence level of I for the long-term success of SCS therapy in randomized controlled trials, compared to conventional medical management and reoperation. In our study, all patients were programmed with tonic stimulation and standard protocol in all patients enrolled. Possibly, other types of waveforms or programming could have had an influence, or have generated other results, which should be a source of future studies in this area.

However, and despite what was previously reported and the level of evidence, the reasons for SCS failure in the reduction of pain scores or the functional

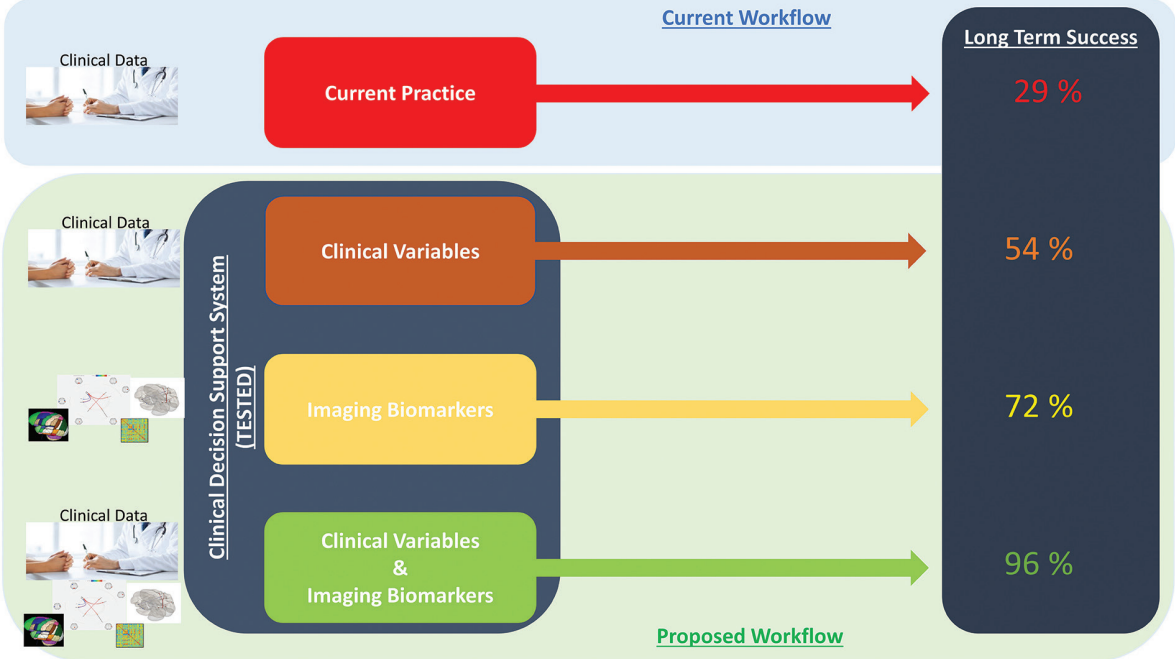

Fig. 3. *Clinical decision support system performance in 3 different scenarios vs current decision workflow.*

		True Value			
	Total Population 24	**Improved Patients**	**Unimproved Patients**	**ACC** 95.83%	
Predicted Value	**Improved Patients**	6	0	**PPV** 100.00%	**FDR** 0.00%
	Unimproved Patients	1	17	**FOR** 5.56%	**NPV** 94.44%
		TPR 85.71%	**FPR** 0.00%	**F1 Score** 92.31%	
		FNR 14.29%	**TNR** 100.00%		

Fig. 4. *Confusion matrix with precision-recall and sensitivity-specificity metrics to fully characterize the classifier's performance.*

TPR, true positive rate, recall, sensitivity; FPR, false postive rate, fall-out; FNR, false negative rate, miss rate; TNR, true negative rate, specificity; AAC, accuracy; PPV, positive predictive value, precision; FDR, false discovery rate; FOR, false omission rate; NPV, negative predictive value

improvement in FBSS patients are still unknown (39). To characterize these mechanisms, objective parameters that could be quantified, such as image biomarkers (3), quantitative sensory testing (QST) (40), evoked compound action potential (ECAP) (40,41), and functional neuroimaging, etc., combined with traditional self reported tests of pain, might improve clinical management, identifying which patients could benefit in the long term from this therapy.

Imaging biomarkers, in addition to current clinical management, were used before in acute stroke (42) and might guide the selection of patients with fMR characteristics who will not benefit from SCS therapy.

The PD-Q is one of the most used questionnaires to detect neuropathic pain and it´s the most useful to reflect improvement after the SCS implant (8). Based on the larger experience of our group in SCS treatment, there were qualitative clinical differences between patients who achieved a 10-point improvement, and those who did not. Thus, we have allocated patients based in this scale to a group of responders to the therapy and a group of nonresponders to SCS.

The physiopathological mechanism involved in the SCS therapy included the segmental action´s mechanism and the supraspinal pathway (43,44). Besides, some studies, have suggested the presence of an altered brain activity in the medial thalamus, the insula, the somatosensory cortex, and the anterior cingulate cortex after SCS (45-47).

Yu et al (48) described a negative correlation between the duration of chronic low back pain and the functional connectivity in the posterior insula and left amygdala. Also, a negative correlation between gray matter volume in the rostral anterior cingulate cortex (rACC), parahippocampus, middle temporal gyrus contralateral to the pain, and ipsilateral right inferior temporal gyrus have been described (18). The disturbances observed in these patients, are related to some cognitive and emotional components, and they probably reflect the lack of adaptation to the patient self-pain level (19). MR and positron emission tomography (PET) have been used to describe the presence of a dopamine increase in the striated nucleus proportional to the augmentation in the pain intensity experimented and the psychological affectation derived from the presence of chronic pain (18). In patients with chronic lumbar pain, fMRI reflects a lower activation of the prefrontal cortex and the nucleus accumbens, with connectivity between the prefrontal cortex and accumbens proportional to the chronicity of the lower back pain (18,36,49). The high connectivity between the medial prefrontal area and the nucleus accumbens could predict the chronicity of pain. Similar associations have been observed in the styles of catastrophization and accompanying depression with little specificity of the pathology (18).

FBSS patients with SCS programmed high density or high dose SCS (HD-SCS) showed brain and brainstem regions modulation of the descending pain modulatory

system, resulting in inhibitory supraspinal effects (47).

In a recent study, results demonstrate that HF-SCS at 10 kHz might influence the salience network and therefore also the emotional awareness of pain. An increased connectivity over time between the anterior insula (affective salience network) and regions of the frontoparietal network and the central executive network were shown. After 3 months of HF-SCS, the increased strength in functional connectivity between the left dorsolateral prefrontal cortex and the right anterior insula was significantly correlated with the minimum clinically important difference (MCID) value of the Pittsburgh sleep quality index (50). These results are confirmed in our study where there was an increased connectivity in the right insula cortex.

Furthermore, a significant correlation was found between the left temporal plane, which regulates certain emotions such as anxiety or anger, and the right insular cortex, which is related to the emotional experience (Table 3). Also, in these patients, a lack of correlation between the anterior right division of the lower temporal turn and the right frontal cortex of the operculum is observed. According to data, the specific impact of each relationship could be explained using Brodmann's interactive atlas, which indicates the known functions of each region.

In our study, we aimed at identifying brain areas involved in the experience of chronic pain and we used that information to propose the application of the imaging biomarkers to facilitate the selection of suitable patients for SCS implant surgery using the imaging biomarkers provided by rs-fMRI and the clinical variables obtained during the first consultation. Hence, these are objective methods for selecting those patients who could obtain a significant improvement with SCS treatment, and they would avoid futility and iatrogenic practices during the trial phase.

As for the feasibility of performing an additional test, brain MRI, although not included in the clinical practice and management of these patients, the cost of the test for the health system and its impact on the patient's quality of life (remember that it is a non-invasive test and harmless for the patient), represent a tiny percentage of total cost when compared to the cost of current treatment for the implantation of a neurostimulator (surgery, cost of the implant, readjustment visit, etc.) and the impact on the patient's quality of life.

Therefore, the major limitation lies in obtaining a large number of homogeneous patients with previous MRI who have followed the same neurostimulator configuration protocols so that the neuroimaging biomarkers and the classification system obtained are as generalized as possible.

Limitations

This study has several limitations that must be considered. First, this is a pilot study and results should be interpreted carefully. Although the best classifier, using the leave-one-out technique, was trained and tested on 24 occasions, of which it failed on only one occurrence, it will be necessary to expand the sample size tol allow for confirmation or rejection of our findings by training the classifier in more patients. Second, the CDSS was designed in the context of a decrease of more than 10 units in the PD-Q, which is an arbitrary cut-off point based in our experience. Third, due to the small percentage of patients in the respondent group (7 patients, 29%), external validation is needed. Also, pain departments with no access to rs-fMRI with advance imaging analysis techniques will not be able to include volumetric and ROI-to-ROI analysis as a part of the selection algorithm for patients with FBSS and with a potential indication for SCS therapy. We acknowledge that image data were available only from patients with FBSS; thus, we could not compare our findings with rs-fMRI studies from control cases.

Conclusions

Five potential findings via imaging biomarkers of a successful response to SCS therapy in FBSS are present in rs-fMRI. The volumetric analysis showed differences in the left putamen, and 4 pairwise brain areas were statistically significant. A CDSS with a diagnostic accuracy of 96% could help physicians select optimal candidates for SCS therapy before the trial phase.

References

1. Simpson EL, Duenas A, Holmes MW, Papaioannou D, Chilcott J. Spinal cord stimulation for chronic pain of neuropathic or ischaemic origin: Systematic review and economic evaluation. *Health Technol Assess* 2009; 13:iii-154.
2. Deer TR, Grider JS, Lamer TJ, et al. A systematic literature review of spine neurostimulation therapies for the treatment of pain. *Pain Med* 2020; 21:1421-1432.
3. De Andrés J, Navarrete-Rueda F, Fabregat G, et al. Differences in gene expression of endogenous opioid

peptide precursor, cannabinoid 1 and 2 receptors and interleukin beta in peripheral blood mononuclear cells of patients with refractory failed back surgery syndrome treated with spinal cord stimulation: Markers of therapeutic outcomes? *Neuromodulation* 2021; 24:49-60.

4. Spinal cord stimulation for chronic pain of neuropathic or ischaemic origin. National Institute for Health and Care Excellence. 2008; Available at: www.nice.org.uk/guidance/ta159. Accessed 11/13/2020.
5. Dworkin RH, O'Connor AB, Kent J, et al. Interventional management of neuropathic pain: NeuPSIG recommendations. *Pain* 2013; 154:2249-2261.
6. Deer TR, Mekhail N, Provenzano D, et al. The appropriate use of neurostimulation of the spinal cord and peripheral nervous system for the treatment of chronic pain and ischemic diseases: The neuromodulation appropriateness consensus committee. *Neuromodulation* 2014; 17:515-550.
7. Cruccu G, Garcia-Larrea L, Hansson P, et al. EAN guidelines on central neurostimulation therapy in chronic pain conditions. *Eur J Neurol* 2016; 23:1489-1499.
8. De Andres J, Monsalve-Dolz V, Fabregat-Cid G, et al. Prospective, randomized blind effect-on-outcome study of conventional vs high-frequency spinal cord stimulation in patients with pain and disability due to failed back surgery syndrome. *Pain Med* 2017; 18:2401-2421.
9. Oakley JC, Krames ES, Stamatos J, Foster AM. Successful long-term outcomes of spinal cord stimulation despite limited pain relief during temporary trialing. *Neuromodulation* 2008; 11:66-73.
10. North RB, Calodney A, Bolash R, et al. Redefining spinal cord stimulation "trials": A randomized controlled trial using single-stage wireless permanent implantable devices. *Neuromodulation* 2020; 23:96-101.
11. Duarte RV, McNicol E, Colloca L, Taylor RS, North RB, Eldabe S. Randomized placebo-/sham-controlled trials of spinal cord stimulation: A systematic review and methodological appraisal. *Neuromodulation* 2020; 23:10-18.
12. Teton ZE, Blatt D, AlBakry A, et al. Natural history of neuromodulation devices and therapies: A patient-centered survival analysis. *J Neurosurg* 2019; 132:1385-1391.
13. Eldabe S, Gulve A, Thomson S, et al. Does a screening trial for spinal cord stimulation in patients with chronic pain of neuropathic origin have clinical utility and cost-effectiveness (TRIAL-STIM)? A randomised controlled trial. *Pain* 2020; 161:2820-2829.
14. Odonkor C, Kwak R, Ting K, Hao D, Collins B, Ahmed S. Fantastic four: Age, spinal cord stimulator waveform, pain localization and history of spine surgery influence the odds of successful spinal cord stimulator trial. *Pain Physician* 2020; 23:E19-E30.
15. Patel SK, Gozal YM, Saleh MS, Gibson JL, Karsy M, Mandybur GT. Spinal cord stimulation failure: Evaluation of factors underlying hardware explantation. *J Neurosurg Spine* 2019; 1-6.
16. Goudman L, Bruzzo A, van de Sande J, Moens M. Goal identification before spinal cord stimulation: A qualitative exploration in potential candidates. *Pain Pract* 2020; 20:247-254.
17. Palmer N, Guan Z, Chai NC. Spinal cord stimulation for failed back surgery syndrome -- patient selection considerations. *Transl Perioper Pain Med* 2019; 6:81-90.
18. Pahapill PA, Chen G, Arocho-Quinones EV, Nencka AS, Li SJ. Functional connectivity and structural analysis of trial spinal cord stimulation responders in failed back surgery syndrome. *PLoS One* 2020; 15:e0228306.
19. Yu R, Gollub RL, Spaeth R, Napadow V, Wasan A, Kong J. Disrupted functional connectivity of the periaqueductal gray in chronic low back pain. *Neuroimage Clin* 2014; 6:100-108.
20. Malfliet A, Coppieters I, Van Wilgen P, et al. Brain changes associated with cognitive and emotional factors in chronic pain: A systematic review. *Eur J Pain* 2017; 21:769-786.
21. Coppieters I, Cagnie B, De Pauw R, Meeus M, Timmers I. Enhanced amygdala-frontal operculum functional connectivity during rest in women with chronic neck pain: Associations with impaired conditioned pain modulation. *Neuroimage Clin* 2021; 30:102638.
22. Lamichhane B, Jayasekera D, Jakes R, et al. Multi-modal biomarkers of low back pain: A machine learning approach. *Neuroimage Clin* 2021; 29:102530.
23. Bossuyt PM, Reitsma JB, Bruns DE, et al. Standards for reporting of diagnostic accuracy. The STARD statement for reporting studies of diagnostic accuracy: explanation and elaboration. *Ann Intern Med* 2003; 138:W1-W12.
24. Diagnostic and Statistical Manual of Mental Disorders. 5th ed. Available from: https://doi.org/10.1176/appi.books.9780890425596. Accessed 11/13/2020.
25. Friston KJ, Zarahn E, Josephs O, Henson RN, Dale AM. Stochastic designs in event-related fMRI. *Neuroimage* 1999; 10:607-619.
26. Unraveling the mysteries of the brain - MIT McGovern Institute. Available from: https://mcgovern.mit.edu/. Accessed 11/13/2020.
27. Abraham A, Pedregosa F, Eickenberg M, et al. Machine learning for neuroimaging with scikit-learn. *Front Neuroinform* 2014; 8:14.
28. Chen QF, Chen HJ, Liu J, Sun T, Shen QT. Machine learning classification of cirrhotic patients with and without minimal hepatic encephalopathy based on regional homogeneity of intrinsic brain activity. *PLoS One* 2016; 11:e0151263.
29. Khosla M, Jamison K, Ngo GH, Kuceyeski A, Sabuncu MR. Machine learning in resting-state fMRI analysis. *Magn Reson Imaging* 2019; 64:101-121.
30. Ben Bouallègue F, Tabaa Y Al, Kafrouni M, Cartron G, Vauchot F, Mariano-Goulart D. Association between textural and morphological tumor indices on baseline PET-CT and early metabolic response on interim PET-CT in bulky malignant lymphomas. *Med Phys* 2017; 44:4608-4619.
31. Treece GM, Gee AH, Tonkin C, et al. Predicting hip fracture type with cortical bone mapping (CBM) in the Osteoporotic Fractures in Men (MrOS) Study. *J Bone Miner Res* 2015; 30(11).
32. Varol E, Sotiras A, Davatzikos C. MIDAS: Regionally linear multivariate discriminative statistical mapping. *Neuroimage* 2018; 174:111-126.
33. Fernández A, García S, Galar M, Prati RC, Krawczyk B, Herrera F. Learning from imbalanced data streams. In: Learning from imbalanced data sets. Springer International Publishing, 2018, pp. 279-303.
34. Benjamini Y., Hochberg Y. Controlling the false discovery rate - A practical and powerful approach to multiple testing. *J R Stat Soc* 1995; Series B. (57):289-300.
35. Vallet R. Pingouin: statistics in Python. *Journal of Open Source Software* 2018; 3:1026.
36. Deogaonkar M, Sharma M, Oluigbo C, et al. Spinal cord stimulation (SCS) and functional magnetic resonance

imaging (fMRI): Modulation of cortical connectivity with therapeutic SCS. *Neuromodulation* 2016; 19:142-153.

37. Frey ME, Manchikanti L, Benjamin RM, Schultz DM, Smith HS, Cohen SP. Spinal cord stimulation for patients with failed back surgery syndrome: A systematic review. *Pain Physician* 2009; 12:379-397.
38. Amirdelfan K, Webster L, Poree L, Sukul V, McRoberts P. Treatment options for failed back surgery syndrome patients with refractory chronic pain: An evidence based approach. *Spine (Phila Pa 1976)* 2017; 42 Suppl 14:S41-S52.
39. Sankarasubramanian V, Harte SE, Chiravuri S, et al. Objective measures to characterize the physiological effects of spinal cord stimulation in neuropathic pain: A literature review. *Neuromodulation* 2019; 22:127-148.
40. Meier K, Nikolajsen L, Sørensen JC, Jensen TS. Effect of spinal cord stimulation on sensory characteristics: A randomized, blinded crossover study. *Clin J Pain* 2015; 31:384-392.
41. Levy R, Deer TR, Poree L, et al. Multicenter, randomized, double-blind study protocol using human spinal cord recording comparing safety, efficacy, and neurophysiological responses between patients being treated with evoked compound action potential-controlled closed-loop spinal cord stimulation or open-loop spinal cord stimulation (the EvokeStudy). *Neuromodulation* 2019; 22:317-326.
42. Puig J, Blasco G, Alberich-Bayarri A, et al. Resting-state functional connectivity magnetic resonance imaging and outcome after acute stroke. *Stroke* 2018; 49:2353-2360.
43. Linderoth B, Foreman RD. Conventional and novel spinal stimulation algorithms: Hypothetical mechanisms of action and comments on outcomes. *Neuromodulation* 2017; 20:525-533.
44. Sivanesan E, Maher DP, Raja SN, Linderoth B, Guan Y. Supraspinal mechanisms of spinal cord stimulation for modulation of pain: Five decades of research and prospects for the future. *Anesthesiology* 2019; 130:651-665.
45. Bentley LD, Duarte RV, Furlong PL, Ashford RL, Raphael JH. Brain activity modifications following spinal cord stimulation for chronic neuropathic pain: A systematic review. *Eur J Pain* 2016; 20:499-511.
46. Kolesar TA, Bilevicius E, Kornelsen J. Salience, central executive, and sensorimotor network functional connectivity alterations in failed back surgery syndrome. *Scand J Pain* 2017; 16:10-14.
47. De Groote S, Goudman L, Peeters R, et al. The influence of high dose spinal cord stimulation on the descending pain modulatory system in patients with failed back surgery syndrome. *NeuroImage Clin* 2019; 24:102087.
48. Yu CX, Ji TT, Song H, et al. Abnormality of spontaneous brain activities in patients with chronic neck and shoulder pain: A resting-state fMRI study. *J Int Med Res* 2017; 45:182-192.
49. Baliki MN, Petre B, Torbey S, et al. Corticostriatal functional connectivity predicts transition to chronic back pain. *Nat Neurosci* 2012; 15:1117-1119.
50. De Groote S, Goudman L, Peeters R, Linderoth B, Vanschuerbeek P, Sunaert S, De Jaeger M, De Smedt A, Moens M. Magnetic resonance imaging exploration of the human brain during 10 kHz spinal cord stimulation for failed back surgery syndrome: a resting state functional magnetic resonance imaging study. *Neuromodulation* 2020; 23:46-55.

Appendix 1.

Programming Protocol:

All patients were programmed following the same guidelines and pursuing the same goal: to maximize the coverage of paraesthesia superimposed on the pain area.

The programming software "Bionic Navigator 1.1 Programming software with Illumina 3D" was used to achieve this goal. The Illumina 3D algorithm optimally selects the anodes and cathodes needed to confine the electric field to a given stimulation point. It works as follows.

1. The algorithm counts different inputs:
   a. Anatomical references concerning the position of the electrode within the spine: vertebral level, mediolateral position of the electrode, and depth of the cerebrospinal fluid.
   b. Type of electrode selected: 8-pole, 16-pole, surgical, etc.
   c. Relative references in terms of the position of one electrode concerning the other: alignments (parallel, offset), spacing.
2. Central Point of Stimulation (CPS). This is reverse-engineered; the user tells the algorithm where the user wants to confine the electric field, configuring the optimal anodes and cathodes to generate the electric field. The CPS concept is based on the point where the electric field will be concentrated to do the stimulation. The software is represented as a green circle with a letter (A) in the middle; below this point is where the stimulation point is confined.

The algorithm is based on a three-dimensional finite element mathematical model (FEM) created for the thoracic part of the spine and its surrounding structures: white matter, grey matter, cerebrospinal fluid, dura, epidural space tissue, the vertebral bone, and the electrodes considering the conductivity, density, and resistivity of each of these structures.

3. To achieve maximum stimulation coverage over the pain area, the following steps followed systematically in each patient:
   3.1. Mimic the actual position of the electrodes (fluoroscopy) within the programming software.
   3.2. On the programming screen, select the CPS at the distal and medial sides of the two electrodes, and sweep under the electrodes. In this sweep, look for an SPC where we have maximum stimulation coverage in the pain zone.
   a) Start with a pulse width of 400μs and in the distal part of the electrode.
   b) Increase the amplitude (mA) until the patient notices the paraesthesias, and when sweeping, adjust the amplitude so that the patient always notices them.
   c) If the patient has good coverage, but a small percentage is missing (toe, lumbar area), increase the pulse width.
4. Once the maximum coverage area has been found and the programming has been adjusted to pleasant paraesthesia, the programming finished. The program was saved.

Appendix 2.

MR Imaging Protocol: Acquisition technique

Magnetic resonance (MR) images were obtained using the 1.5T MR system (Ingenia, Philips, Best, The Netherlands) with 8-channel head coil according to the approved settings/recommendations for SCS devices.

Transverse MR images were acquired parallel to the anterior commissure and posterior commissure plane with the following sequences:

T1 weighted high-resolution gradient echo (GRE) sequence (3D-T1w-GRE): TE/TR=4.6/9.5 ms, voxel size=0.48 x 0.48 x 1.00 mm, acquisition matrix= 512 x 512 x 170, flip angle=16°. These images were used to parcellate brain regions and for the voxel-base morphometry (VBM) analysis.

Resting-state functional MR (rs-fMR) blood oxygenation level–dependent BOLD MR (rs-fMR) imaging with a T2* weighted Echo Planar Imaging (EPI) sequence with continuous acquisition: TE/TR = 50 / 2750 ms, voxel dimensions=3.59x3.59x4 mm, acquisition matrix = 64 x 64 x 30, dynamic blocks = 135, total acquisition time was 6-minutes. The patients were instructed to keep their eyes close during all the sequence acquisition.